Optimizing Ultrasonic Intensity for High Intensity Focused Ultrasound Therapy

BEE4530
Computer Aided Engineering: Application to Biomedical Process

Group 5
Matt Carter
Art Sullivan
Kenny Byers
Michael Jessel

Table of Contents

Acknowledgements

The authors gratefully acknowledge Dr. Ashim K. Datta, Cornell University Biological and Environmental Engineering Professor, for his advice and guidance helping define our problem and understand ultrasound physics. We thank Alex Warning, graduate student in Cornell's Department of Biological and Environmental Engineering, for his invaluable expertise in modeling and adapting physics in COMSOL. Finally, we thank Dr. Traci Nathans-Kelly for her advice on presenting our information in a clear and compelling manner.

I | Executive Summary

Every year as many as one million individuals worldwide are diagnosed with hepatocellular carcinoma (HCC), the most common form of liver cancer. Caused by cirrhosis, HCC is typically treated with surgery or chemotherapy. High intensity focused ultrasound (HIFU) therapy, an emerging treatment option, is a noninvasive alternative to these methods.

HIFU targets a cancerous tumor and induces necrosis while reducing damage to surrounding tissue. Acoustic pressure waves propagate from a curved transducer head into the tissue medium. The curved nature of the transducer surface focuses the pressure waves into a selected region and the energy of the beam is converted into heat. HIFU allows for precise targeting of tumor regions and reduced necrosis of healthy tissue. It is easier to control the depth and position of interstitial ultrasound than it is for other interstitial heating methods, such as percutaneous ethanol injection and radiofrequency.

This project models the treatment of liver cancer using HIFU therapy. We model the thermal necrosis of a liver tumor caused by an ultrasonic transducer, and we optimize the process to maximize tumor ablation and minimize tissue damage. The process is modeled in COMSOL Multiphysics using 2-D axisymmetric coordinates which simplifies the tumor geometry as symmetric and includes the HIFU probe and surrounding tissue. Transducer size and parameters are that of the JC-model HIFU transducer from Haifutech, Inc. Relevant tumor and tissue parameters are taken from the literature. Pressure waves are modeled using the Helmholtz equation and heat transfer utilizes the Bioheat Equation. Tumor and tissue ablation are evaluated with a thermal dose equation.

Our results show pressure wave propagation focused at the center of the liver tumor. Maximum heating occurs at the tumor center where pressures were the highest and lower temperatures are seen in healthy tissue regions, indicating a proper coupling of the ultrasound and heat transfer physics. A transducer frequency of 1 MHz with a power of 200W and a sonication time of 3.2 seconds maximizes tumor ablation while minimizing healthy tissue damage in a 0.8 cm diameter tumor.

This model demonstrates the effective heating of HCC tumors by HIFU, and can be used as a reference for optimizing a heating dose for tumors of known sizes.

II | Introduction to Hepatocellular Carcinoma and HIFU Therapy

Hepatocellular carcinoma (HCC), also called malignant hepatoma, is the fifth most common form of cancer worldwide and the most common form of liver cancer [1]. As many as one million new cases occur worldwide each year [2]. In 80% of cases, HCC is caused by cirrhosis, a gradual scarring of the liver tissue that ultimately results in loss of organ function. Typically, alcoholism, hepatitis, inflammation, or excessive iron levels induce cirrhosis in humans [3]. The preferred cure for HCC is surgery, but this is not possible for many patients. In fact, only between 10-20% of hepatocellular carcinomas can be removed by surgery. Other options such as chemotherapy and radiation treatment are possible, but both can produce severe adverse effects. Furthermore, depending on the degree of cirrhosis, radiation treatment may not be possible at all [3]. If carcinomas cannot be successfully removed or destroyed, the disease is usually deadly within three to six months.

High intensity focused ultrasound (HIFU) is a less invasive alternative therapy that can treat HCC. HIFU therapy is currently viewed as an experimental therapy in the United States and most of the research has been done in China and the UK. HIFU is able to treat HCC via hyperthermic ablation of liver tumors. A HIFU transducer generates ultrasonic waves that focus to a point. The ultrasonic waves are partially absorbed as they propagate through the tissue, which leads to heating. The heating is greatest in the focal region of the ultrasonic propagation field. After each thermal exposure, the transducer can be adjusted to strike a new location on the tumor and treat an entire malignant mass regardless of geometry [4]. In HIFU treatment, thermal exposures are typically under 10 seconds. Ideally, temperatures within the tumor reach temperatures in excess of 54 °Celsius in order to induce tissue ablation. Additionally, it is desirable to avoid excess heating of the surrounding healthy tissue to reduce the risk of complications to the treatment [5].

In this report, we model our HIFU transducer after the JC-Model transducer from Haifutech, Inc. [6]. In practice, the patient lays on top of a table attached to a basin of degassed water, seen in **Figure 1**. The transducer sits in this basin of water. The water is necessary because ultrasonic waves require a medium to propagate through before entering the tissue [8].

Figure 1. *The JC-Model Haifu System. The patient lies on top of the platform that is attached to a basin of water, which is boxed in red. The transducer sits inside this basin of water and is oriented such that the focal point of the transducer is aimed at the patient's tumor [7].*

In order to model heating of liver and tumor tissue we must incorporate the physics of the ultrasonic waves. The heat transfer physics and acoustical physics will thus be coupled in our computational model. Sonication of the tissue will take place over a span of 0 to 10 seconds with a frequency of 1 MHz. We will vary the power level of the ultrasonic transducer in order to optimize destruction of tumorous tissue while minimizing damage to healthy tissue.

III | Problem Statement Pertaining to Model Objective

No model currently exists for optimizing ultrasonic intensity of HIFU treatment of liver tumors. A model would be useful in understanding the physics of this treatment, and would assist in the design process by maximizing the amount of tumor ablated while minimizing damage to healthy surrounding tissue.

IV | Design Objectives for Optimized Solution

1. Model thermal necrosis of a hepatic tumor caused by an ultrasonic transducer in 2D for a range of intensities.
2. Optimize the intensity of the transducer to maximize tumor ablation and minimize healthy tissue damage.

V | Design Schematic of Transducer and Tissue Geometries

A qualitative depiction of the HIFU process can be found in **Figure 1A.** The curved ultrasonic transducer's surface causes the waves converge at a focal point, which is located in a tumor within the liver. The bulk of the heating in the tissue due to the attenuation of the ultrasonic waves should occur in this focal region.

In order to successfully model this process, we need to include the surface of the transducer, the water region, the tissue region and the tumor region. We modeled this entire domain in 2-D axisymmetric geometry, as demonstrated in **Figure 1B**. The transducer surface is shown in red. Note that the transducer itself cannot be seen, we simply needed to model the boundary. The apparatus to the left of the transducer surface is used to model a hole in the center of the transducer. In a clinical setting, an imaging probe is usually placed in this hole.

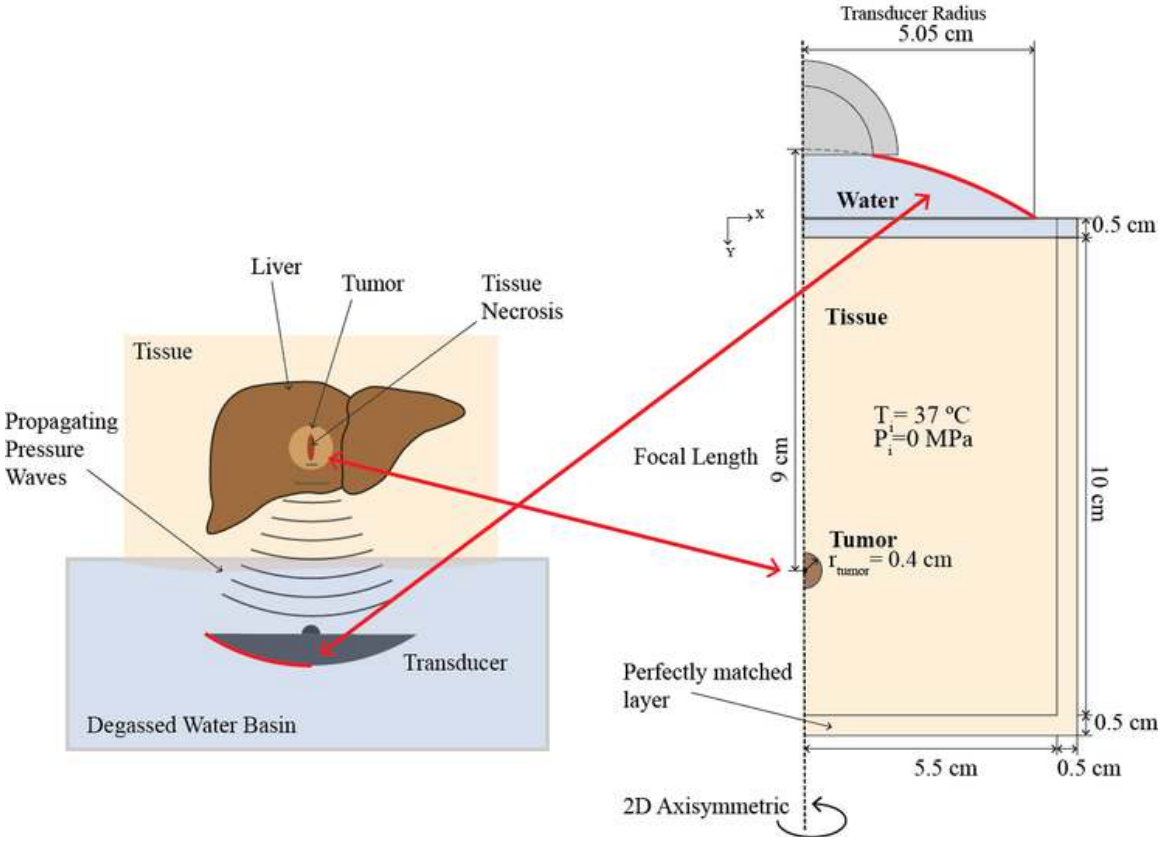

Figure 1. *A) Qualitative representation of the high intensity focused ultrasound showing waves propagating from a transducer head to the hepatic tumor through a layer of water, a layer of tissue, and the liver. B) Geometry of the HIFU model used in this report. It is composed of the transducer surface (shown in red), a water domain, a tissue domain and a tumor domain. The transducer itself cannot be seen. The quarter-circle to above and to the left of the transducer surface is present to model a hole in the center of the transducer.*

Around the edge of the water and tissue domains is a perfectly matched layer boundary condition. This layer absorbs the pressure waves and truncates the acoustic propagation domain such that waves do not reflect off the outer boundaries. This boundary condition

reflects the clinical situation, in which the waves dissipate into the body. Ultrasonic waves are mechanical pressure waves, and so the boundary condition on the surface of the transducer head is a pressure flux boundary condition. More information on boundary conditions can be found in **Appendix A Section B**.

In executing this optimization model, it was necessary to make several simplifications to the geometry and physics in order to reduce computational intensity.

- The tumor is assumed to be a perfect sphere
- The tissue surface is considered to be flat
- The tissue is assumed to homogeneous in terms of material properties
- Acoustic waves are assumed to propagate linearly (meaning they propagate at a single frequency)
- The tumor and tissue are assumed to have the same material properties
- Material property values do not change with temperature.

VI | Results

A. Preliminary Results of Running Model

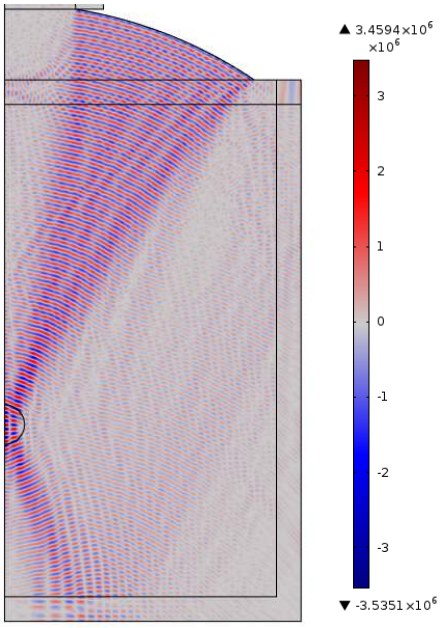

Figure 2. *Propagation of pressure waves in tissue sample. The colored axis is in units of MPa.*

Solving the Helmholtz equation in COMSOL 4.3b using pressure as the dependent variable produced linear wave propagation within the domain, shown in **Figure 2**. Note how the ultrasonic pressure waves emanate from the curved transducer surface and are focused to within the tumor domain. The peak pressures achieved are on the order of 3.5 MPa. A pressure flux boundary condition was set on the transducer surface. This flux was equivalent to $-\omega^2 d_0$ where ω is the frequency of the transducer and d_0 is the displacement amplitude of the transducer head. The frequency used was 1 MHz. The displacement amplitude is derived from the power of the ultrasonic transducer. By altering the displacement amplitude we are essentially altering ultrasonic power. See **Appendix A Section A** for more on this relationship.

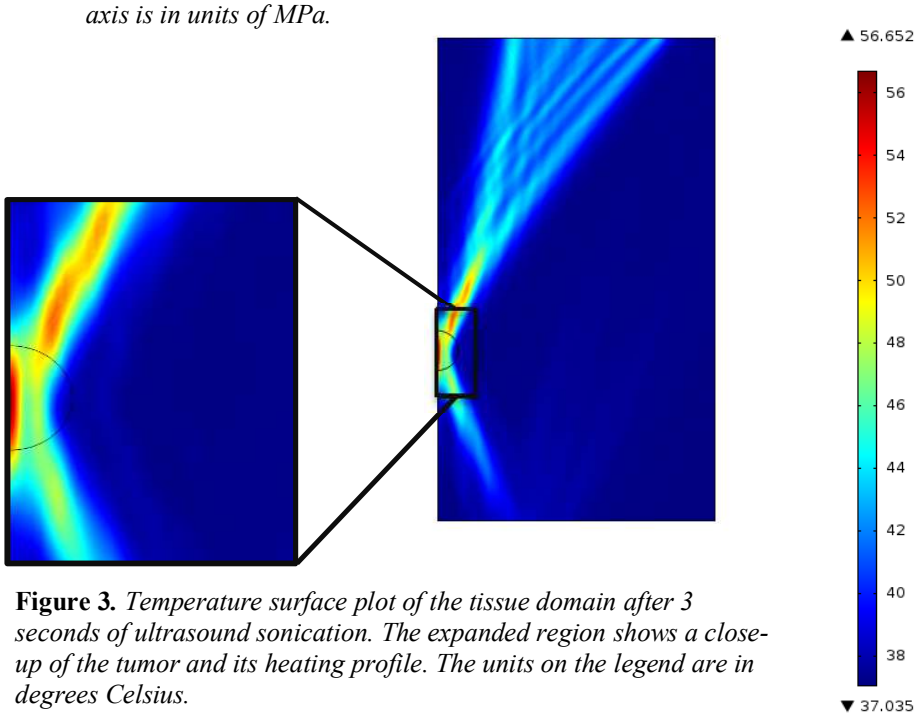

Figure 3. *Temperature surface plot of the tissue domain after 3 seconds of ultrasound sonication. The expanded region shows a close-up of the tumor and its heating profile. The units on the legend are in degrees Celsius.*

In this example the displacement amplitude was set to 100 nm, which correlates to a power of 120 W. The intensity of the transducer in this example is then 1.48 W/cm^2 because power is intensity over the surface area of the transducer head. The area of the transducer head is constant, thus, when we refer to altering ultrasonic power levels, this is akin to varying ultrasonic intensity levels. Note that there is a hole in the center of our transducer and hence there is no wave propagation in the center of the tissue domain.

The wave propagation produced a clear path from transducer head to tumor center, shown in **Figure 2.** The heat generation terms coupled with the wave propagation produced a thermal profile within the wave path, shown in **Figure 3**. Furthermore, the hottest temperature of 56.6 degrees Celsius occurs in the center of the tumor.

B. Optimization of Ultrasonic Intensity and Thermal Dose

We defined our objective function, J, such that ablation of tumor tissue is maximized and damage to healthy tissue is minimized.

$$J = 5 * Volume\ of\ tumor\ ablated - Volume\ of\ liver\ damaged$$

The value of this function varies over time as volumes of tumor ablation and tissue damage increase. The objective function increases as the volume of tumor ablation increases, and it decreases when the volume of healthy liver damage increases. The maximum of this function represents the optimal time of sonication for a given HIFU intensity. The tissue is considered to be *ablated* at 340 CEM_{43}, or 340 cumulative equivalent minutes at or above 43 ^{0}C. The tissue is considered to be *damaged* at 240 CEM_{43}, or 240 cumulative equivalent minutes at or above 43^{0}C. Thus, the thermal ablation threshold is higher than the thermal damage threshold. To preserve the integrity of healthy tissue as much as possible, we track thermal damage rather than simply ablation of healthy tissue. Also note that the volume of tumor ablated is weighed higher than the volume of liver damaged because we consider eliminating the tumor to be more important than damaging an equal volume of healthy tissue.

Figure 4A shows that our objective function is bimodal with one small peak and one larger peak. **Figure 4B** characterizes the amount of damage in and around the tumor at various time points in the heating process that creates the objective function found in **Figure 4A.** The first, smaller peak occurs when all of the thermal damage is in the tumor region. However, as damage begins to occur outside the healthy tissue without an appreciable increase in tumor damage, the objective function decreases. The objective function increases to its global maximum when thermal damage again increases, outpacing damage to the healthy tissue. Finally, the function decreases as more healthy tissue is damaged with less relative tumor ablation.

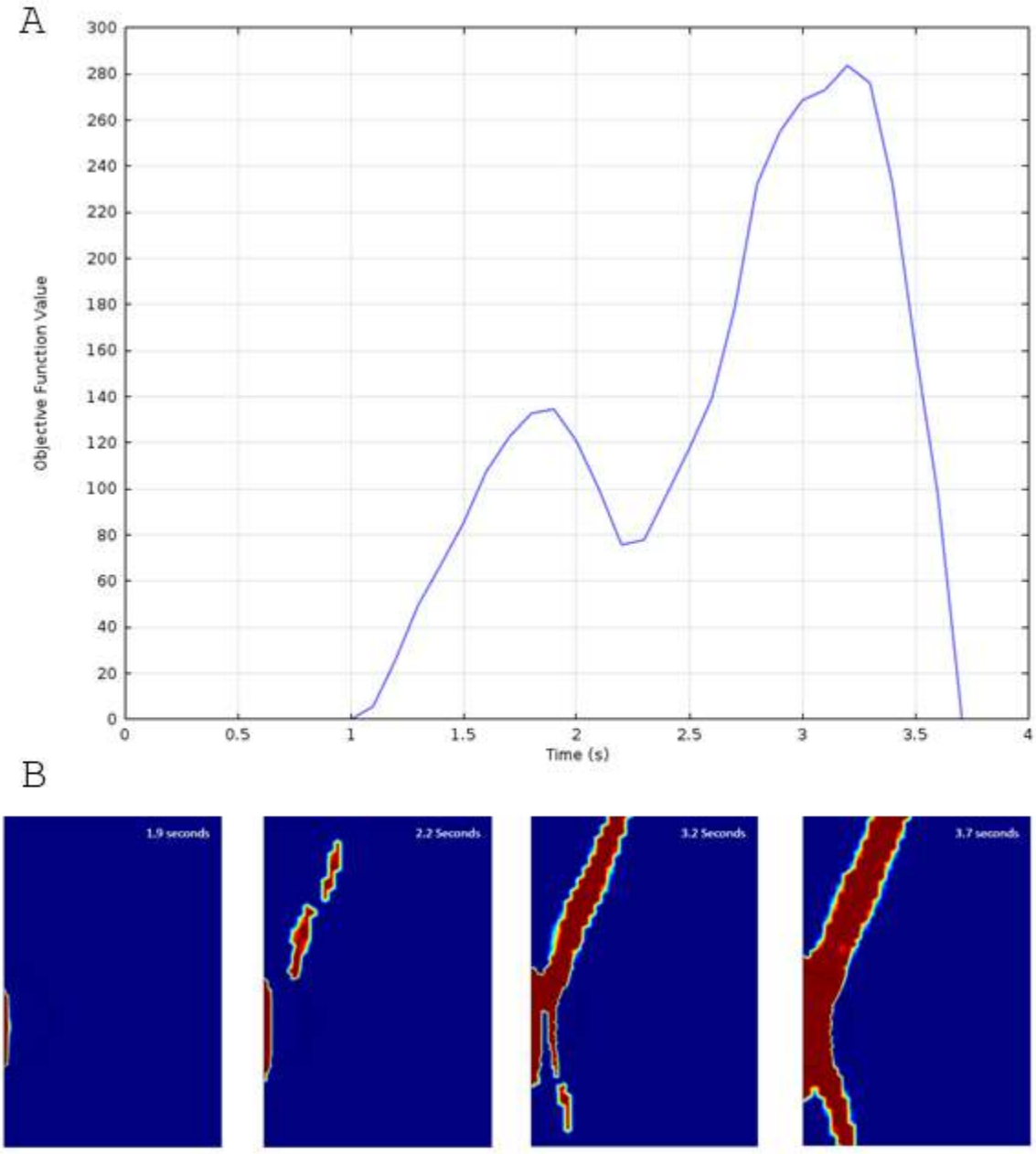

Figure 4. *A) A plot of our objective function when the transducer power was 200W. Note that the function is bimodal in nature. The objective function reaches at peak at 3.2 seconds. This maximum indicates that the maximal amount of tumor has been destroyed, given how much healthy tissue has been damaged. B) Corresponding snapshots of the amount of thermal damage in the tumor and tissue domains at various time points during heating. Red indicates thermal ablation. The tumor is represented by the semi-circles. A time of 1.9 seconds corresponds to the smaller peak in the objective function. The trough in the objective function occurs at 2.2 seconds.. The global maximum in the objective function occurs at 3.2 seconds. The objective function equals zero at a time of 3.7 seconds.*

Plotting multiple objective functions for various power levels allows us to compare different transducer head intensities. **Figure 5** shows an example of such a process. Looking at the figure below, we see that each curve reaches a different global maximum. If we were to plot many objective functions for many different power values, we could find the overall maximum value possible for our objective function and at which power and time this value occurs. This would be the optimal power to use for a HIFU therapy under the conditions that we are modeling.

Generating these objective functions is computationally intensive and can take hours to run on even high end computers. Due to time constraints, we restricted our optimization to four power levels. While not exhaustive, the four data points produced a range of a qualitative overview of objective function optimization. A power level of 200 W results in an optimal objective function value based on the values we have calculated. The 200 W power level correlates to an intensity of 2.46 W/cm^2. It should be noted that increasing power level is associated with decreasing the optimal sonication time. It makes sense that lower power levels would need to heat the tissue for longer periods of time.

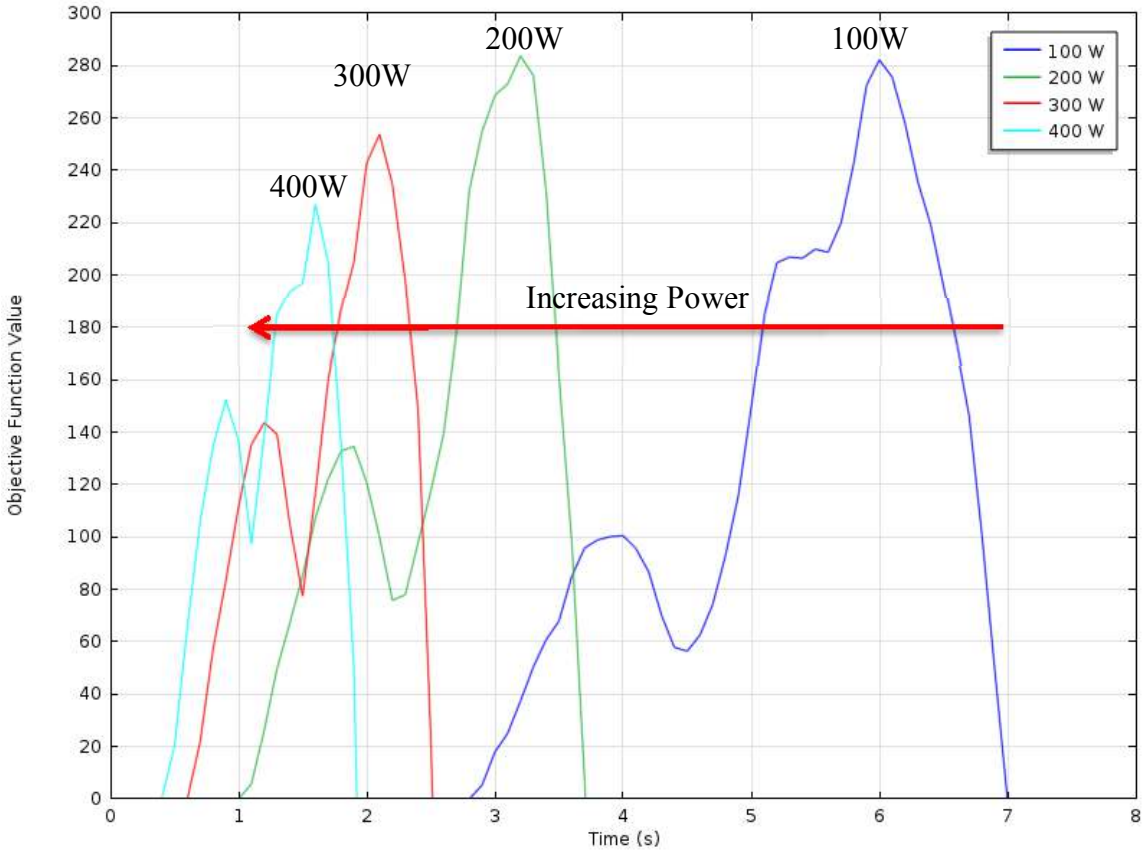

Figure 5. *The objective functions of 4 different ultrasonic power levels are shown. The range of power levels that can be used by the JC-Model Haifutech transducer is between 0 and 400 W. The four power levels chosen (100 W, 200 W, 300 W, and 400 W) thus provide an ample distribution across this range. Note that the time associated with the maximum of the objective function decreases as power increases. Also note that the maximum value of the objective functions also appear to decrease when higher power levels are used.*

C. Validation of Temperature Increase at the Focal Point

We compared our results to another computational model of the JC-Model transducer for validation purposes [9]. The paper used for comparison includes a graph of the temperature rise at the transducer's focal point over time, which was convenient to obtain using our model. We changed our model's transducer head frequency and acoustic power level to match the values used in the Wang paper (1.6 MHz and 50 W, respectively). As seen in **Figure 6** below, the models matched qualitatively and had similar behaviors for temperature rise at the focus. However, the focus in the comparison model has a temperature increase of around 100 degrees Celsius, while our model only increases 3.2 degrees.

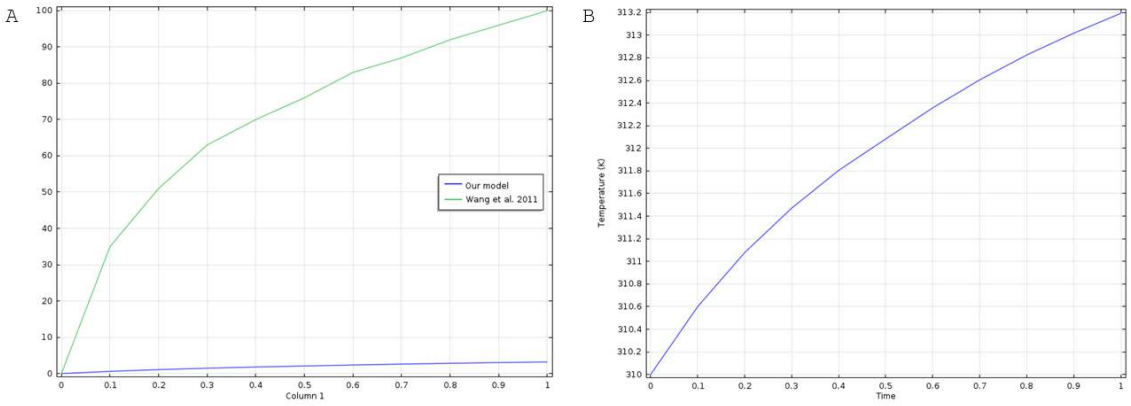

Figure 6. *A) Results of the Wang study increased to 100˚C after 1 second of heating compared to just 3.2 °C for our model. B) The shape of the heating in our model is similar to that for the Wang study, shown by the green line in figure A. This indicates that the pattern of heating in the tumor is the same in both models.*

There are several possible reasons for this quantitative difference in results. First, the comparison paper uses nonlinear wave propagation while our model uses linear wave propagation. Also, the Wang paper does not include information about various parameters for heating calculations. Values such as tissue density, attenuation coefficients, and tissue geometries are not included in the paper. This makes it difficult to replicate the model they created. Finally, this paper looks at experimental heating data from cow livers, but does not explicitly state whether or not their model is for cows or humans.

These factors make it difficult to directly compare results in a quantitative way. However, we can see that the physical behavior is similar when viewed qualitatively. This leads us to believe that our model is valid.

D. Sensitivity Analysis of Focal Temperature

For our sensitivity analysis, we tested how sensitive our results were to two key parameters: attenuation coefficient and the speed of sound through the tissue.

1. Attenuation Coefficient

The attenuation coefficient is central to the coupling of the acoustics governing equation and the bioheat transfer governing equation because the attenuation coefficient is present in the source term of the bioheat transfer equation. We have yet to find data indicating that the tumor tissue and healthy tissue have different attenuation coefficients. Because of this, we will continue to model the tissue domain as having the same attenuation coefficient.

A range of values for the attenuation coefficients for human tissue was discovered in scientific literature [10]. The highest value found was 33 m^{-1} and the lowest value found was 8 m^{-1}. We used these values for the upper and lower limits of the set of values we used in our sensitivity analysis. A parametric sweep was carried out where we tracked the average temperature of the tumor against the various attenuation coefficients over a sonication time of 10 seconds. Higher attenuation coefficient values lead to greater values for average tumor temperature, shown in **Figure 7**. This makes sense given that the attenuation coefficient is directly proportional to the ultrasonic source term in the bioheat transfer, as shown in **Appendix A Section A**. This relationship also explains why average tumor temperature appears to vary linearly with respect to attenuation coefficient. These results show that our model is highly sensitive to changes in the attenuation coefficient. The value that we settled on was 8.55 m^{-1} as this value was corroborated by several papers [11].

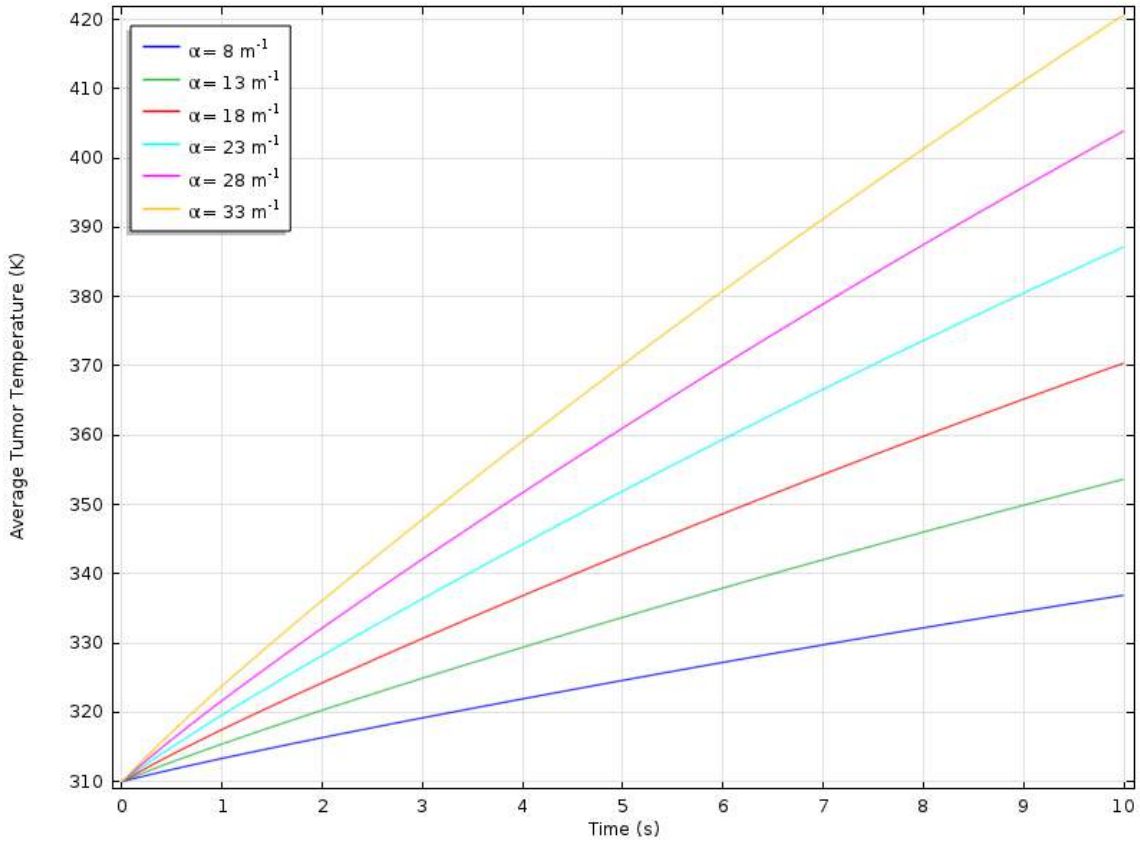

Figure 7. *Average temperature of the tumor domain over time with varying attenuation coefficients, α. The attenuation coefficient measures the extent to which a wave is absorbed by a medium as the wave travels. Thus, higher attenuation coefficients lead to greater temperature in the tumor since the tissue absorbs more energy from the wave. The temperature in the tumor appears to vary linearly with the attenuation coefficient. This makes sense given that the attenuation coefficient α is directly proportional to heating in the equation $Q=2\alpha I$.*

2. Speed of Sound

We also analyzed the sensitivity of our model to the speed of sound in the tissue domains. The speed of sound affects the manner in which waves propagate through the tissue medium and thus affect the pressure distribution in the tissue. In scientific literature, the highest value we found for speed of sound through tissue was 1630 m/s [10]. We did not choose a value smaller than our initial value because the number of elements in our tissue domain is inversely correlated with speed of sound. If we were to decrease the speed of sound it would result in the need for a finer mesh, which was infeasible from a computational standpoint. **Figure 8** demonstrates that varying speed of sound does not appear to have a strong effect on average tumor temperature. **Figure 8** tracks average tumor temperature through the first 10 seconds of heating. This is because we wanted to track this parameter during times when heating was focused on the tumor, rather than when healthy tissue heating would play a larger role in later times.

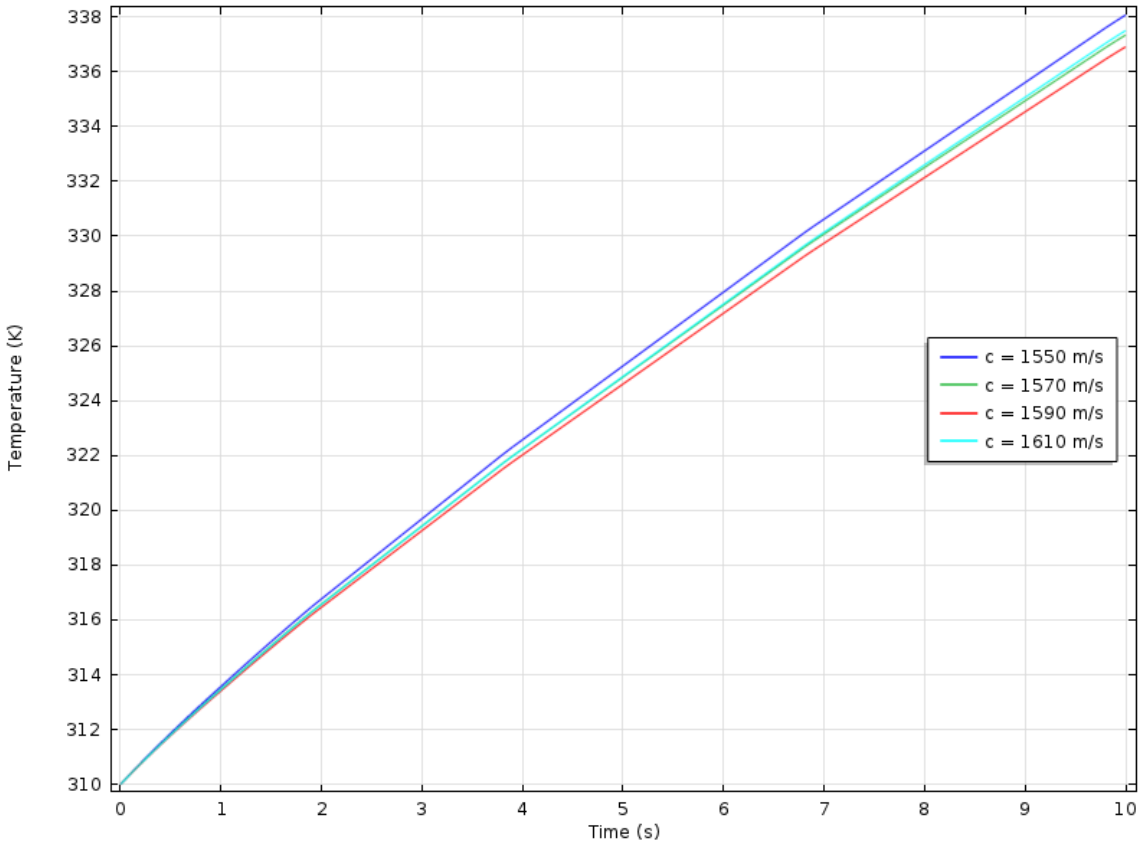

Figure 8. *Average temperature of the tumor domain over time with varying speeds of sound of the ultrasonic waves, c, through the tissue domain. The speed of sound through the tissue affects the pressure wave distribution in the tissue and thus has the potential to impact heating behavior during sonication. The average tumor temperature does not appear to vary significantly with variation in speed of sound during the sonication period we tracked (10 seconds).*

VII | Design Recommendations and Conclusion

We modeled the thermal necrosis of a hepatic tumor caused by an ultrasonic transducer with a focal length of 9 cm. We then optimized the intensity of the transducer head to maximize tumor ablation and minimize healthy tissue damage. To accomplish these goals, we coupled bioheat transfer with acoustic wave propagation in a 2D axisymmetric domain. We checked the sensitivity of two parameters, absorption coefficient and speed of sound through the tissue, and found that the average temperature of the tumor is sensitive to the attenuation coefficient and not sensitive to the speed of sound through the tissue. Next, we validated our model by comparing the physics qualitatively with a previous modelling experiment using the transducer we modeled.

Our objective function allows us to weigh the amount of tumor ablated relative to the amount of healthy tissue damaged for a given intensity and time. Therefore, we are able to use our model to find an optimal heating time for a specified intensity. A power of 200W with a sonication time of 3.2 seconds maximizes tumor ablation while minimizing tissue damage. This power corresponds to an intensity of 2.47 W/cm^2. Taking this further, we can use our function to find the maximum objective value for a range of intensities, which would allow us to find an overall optimal intensity and the associated optimal time for a specific procedure. Computing these objective functions were out of our reach due to limitations in our computational resources, but it is a promising area of future research. We could further contribute to this field by modeling and optimizing the intensities of various other ultrasound transducers and procedures. For example, we could model a different HIFU transducer for hepatic tumor ablation or an ultrasound transducer used for the treatment of breast or prostate cancer. Our model produces results that are useful in medical scenarios and has the potential to optimize a variety of ultrasonic procedures.

VIII | Appendix A: Model Design

A. Governing Equations

Heat transfer in the tissue is governed by the Bioheat Equation as seen in Dillenseger, et al.[4]:

$$\rho_t C_t \frac{\partial T}{\partial t} = k_t \left(\frac{\partial^2 T}{\partial x^2} + \frac{\partial^2 T}{\partial y^2}\right) + V\rho_b C_b (T_b - T) + Q_m + Q_r \quad \{1\}$$

Where ρ_t and C_t represent the density and specific heat of the tissue. $k_t \nabla^2 T$ governs the thermal diffusion through the tissue with k_t being the thermal conductivity of the tissue. $V\rho_b C_b (T_b - T)$ models the effect of perfusion with V being the perfusion rate per unit of volume through the tissue. ρ_b, C_b, and T_b represent, respectively, the density, specific heat and temperature of the blood. The metabolic heat generation term, Q_m, is defined as a constant input parameter.

In order to solve Equation 1, the heat source term from the ultrasonic heating, Q_r, must be determined. It is given by the equation:

$$Q_r = 2\alpha I \quad \{2\}$$

Where α is the attenuation coefficient of the tissue and I is the intensity of the ultrasonic wave, defined as [12]:

$$I = \sqrt{I_z^2 + I_\phi^2 + I_r^2} \quad \{3\}$$

In 2-D axisymmetric coordinates, I_z, I_φ, and I_r are the wave intensities in the axial, angular and radial directions, respectively. These component intensities can be calculated at every point in the domain by taking the dot product of the pressure and the particle velocity. Note that pressure is a scalar term and the article velocities are vector quantities:

$$\boldsymbol{I_z} = 0.5 * (p \cdot \boldsymbol{v_z}) \qquad \boldsymbol{I_\phi} = 0.5 * (p \cdot \boldsymbol{v_\phi}) \qquad \boldsymbol{I_r} = 0.5 * (p \cdot \boldsymbol{v_r}) \quad \{4\}$$

Where the particle velocity in the axial, angular and radial directions are defined as:

$$v_z = -\frac{\frac{dp}{dz}}{(\rho_c * i * \omega)} \qquad v_\phi = -\frac{\frac{dp}{d\phi}}{(\rho_c * i * \omega)} \qquad v_r = -\frac{\frac{dp}{dr}}{(\rho_c * i * \omega)} \quad \{5\}$$

For v_z, dp/dz is the change in pressure with respect to the z coordinate and i is the imaginary number, and ω is the angular frequency of the sound wave (given by the term $2\pi f$, with f being signal frequency). Particle velocity in the radial and angular directions, v_r and v_{phi}, are obtained by substituting the derivative of pressure with respect to radius and angle, respectively. The complex density ρ_c is dependent on the tissue density, speed of sound in tissue, and the complex speed of sound c_c:

$$\rho_c = \rho_t * \left(\frac{c_0}{c_c}\right)^2 \quad \{6\}$$

In equation 6 c_c is the complex speed of sound, defined as:

$$c_c = \frac{\omega}{k} \quad \{7\}$$

Where c_0 is the signal sound speed. The wave moves in the k direction, defined in [m^{-1}] as:

$$k = \left(\frac{\omega}{c_0}\right) - (i * \alpha) \quad \{8\}$$

Note that Equation 3 shows how intensity can be expanded into an analytical expression.

In order to solve the series of equations yielding intensity in equation 3, the pressure produced by the acoustic wave must defined throughout the water and tissue domain. The governing equation for the non-linear propagation of the pressure wave is given by the wave equation [13]:

$$\frac{1}{\rho_0 c^2}\frac{\partial^2 p}{\partial t^2} + \nabla \cdot \left[-\frac{1}{\rho_0}(\nabla p - q)\right] = Q_p \quad \{9\}$$

In the wave equation q and Q_p are possible acoustic dipole and monopole source terms. For our model are both equal to zero, reducing to:

$$\frac{1}{\rho_t c^2}\frac{\partial^2 p}{\partial t^2} + \nabla \cdot \left[-\frac{1}{\rho_0}(\nabla p)\right] = 0 \quad \{10\}$$

The pressure, p, can be expanded into harmonic components using the Fourier series:

$$p * \sin(\omega t) \quad \{11\}$$

This pressure can be written more generally as a complex variable:

$$p = p(x) * e^{i\omega t} \quad \{12\}$$

Solving Equation 10 with this complex variable yields the Helmholtz equation:

$$\nabla \cdot \left(-\frac{1}{\rho_t}\nabla p\right) - \frac{\omega^2}{\rho_t c^2} p = 0 \quad \{13\}$$

COMSOL solves this equation for pressure to produce the acoustic wave that induces heating in the tissue. Solving Equation 13 in the domain determines the pressure at every point over time, thereby allowing heating generation to be obtained at every point.

Changing the displacement amplitude of the transducer, ξ, changes the power and intensity of the transducer. Displacement amplitude relates to power, P, and intensity, I, in the following way:

$$P = \frac{I}{A} = \frac{\xi^2 \omega^2 Z}{A} \quad \{14\}$$

Where Z is the acoustic impedance of the medium the wave is propagating through and A is the area of the transducer head. The acoustic impedance of water is used when determining the intensity of the transducer head. Impedance is equivalent to the product of the density of the medium and the speed of sound through that medium.

Tumor and tissue damage are evaluated as a thermal dose, dependent on the temperature relative to 43ºC, shown by Bailey et al [14]. To cause thermal damage to the tissue, an equivalent heating period of 240 minutes at 43 ºC is required. High temperatures can reach an equivalent dose over much shorter time periods.

$$TD = \int_0^t R^{43-T(t')} dt' \quad \{15\}$$

$$R = \begin{cases} 0.5 \ \ for\, T > 43°C \\ 0.25 \ \ for\, T < 43°C \end{cases}$$

This objective function will be utilized in implementing our objective function in order to quantify the results of our optimization.

$$J = 5 * \iiint_V TD_{tumor} dV - \iiint_V TD_{healthy} dV \quad \{16\}$$

Thermal dose is dependent on temperature, as seen in Equation 5. In turn, temperature is dependent on pressure which is dependent on the frequency of the ultrasonic transducer. Thus, the optimal frequency to use in HIFU treatment is the one that maximizes the objective function J which increases when the volume of tumor tissue ablated increases and decreases when the volume of damaged liver tissue increases. The thermal dose threshold for thermal ablation is higher than for damage. Tissue is considered ablated when the thermal dose reaches 340 equivalent minutes of heating at 43 °C and tissue is considered damaged when the thermal dose reaches 240 equivalent minutes of heating at 43 °C.

B. Boundary Conditions

Figure 9 shows the heat transfer and acoustics domains of our model.

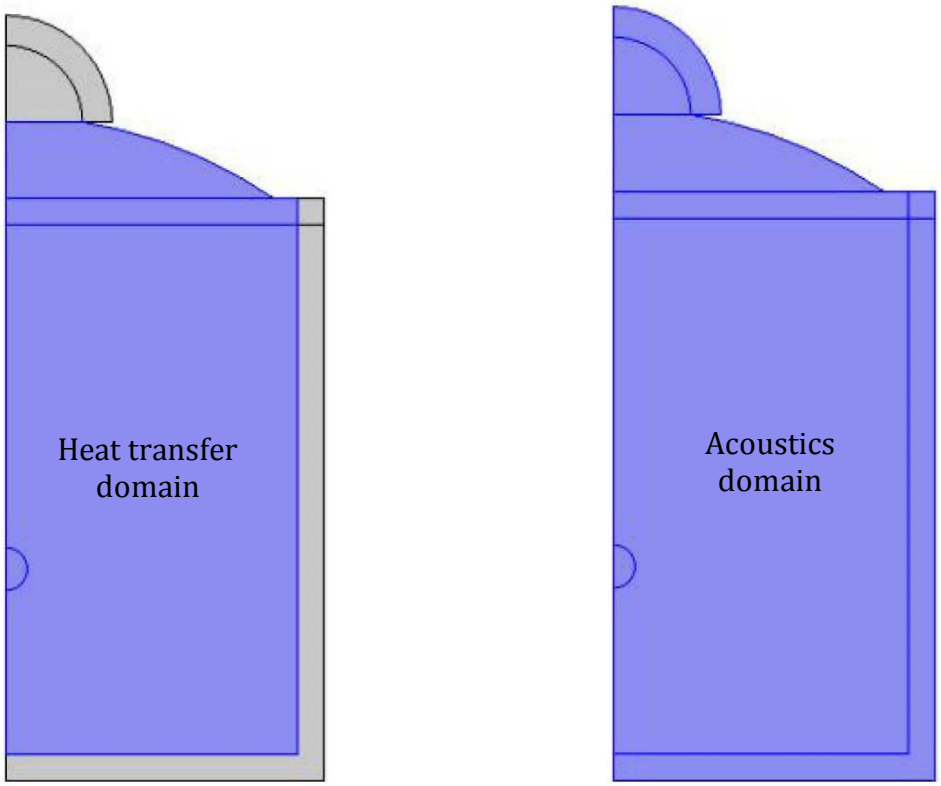

Figure 9. *The image on the left shows the heating domain for the model in blue; the regions in grey are not included in the heating domain. The image on the right shows the pressure domain.*

The heating domain is thermally insulated at all tissue and water boundaries. The right and bottom boundaries have perfectly matched layer boundary conditions. This boundary condition absorbs incoming pressure waves and prevents internal reflection. The transducer boundary is set to have a pressure flux equal to $\omega^2 d_0$, where ω is the angular frequency and d_0 is the displacement amplitude. All other surfaces have a pressure flux of zero.

C. Initial Conditions

The water and tissue domains will have an initial temperature value of body temperature, 310.15 K and an initial pressure of 0 Pa.

D. Input Parameters

Table 1 - A list of the parameters used in our model

Parameter	Description	Value	Source
$\boldsymbol{\rho_t}$	Density of tissue	$1055\ kg/m^3$	[15]
$\boldsymbol{C_t}$	Specific heat of tissue	$3600\ J/kgK$	[15]
$\boldsymbol{k_t}$	Thermal conductivity of tissue	$0.512\ W/mK$	[15]
$\boldsymbol{V}$	Perfusion rate per unit volume of blood	$0.000471\ s^{-1}$	[15],[16]
$\boldsymbol{\rho_b}$	Density of blood	$1060\ kg/m^3$	[15]
$\boldsymbol{C_b}$	Specific heat of blood	$3770\ J/kgK$	[15]
$\boldsymbol{\alpha_t}$	Absorption coefficient of tissue	$8.55\ 1/m$	[12]
$\boldsymbol{\alpha_w}$	Absorption coefficient of water	$0.025\ 1/m$	[12]
$\boldsymbol{c_0}$	Speed of sound in tissue	$1550\ m/s$	[15]
$\boldsymbol{c_w}$	Speed of sound in water	$1483\ m/s$	[12]
$\boldsymbol{f}$	Frequency of sound wave	$1\ MHz$	[12]
$\boldsymbol{T_b}$	Body temperature	$310.15\ K$	[15]
$\boldsymbol{\rho_w}$	Density of water	$1000\ kg/m^3$	[12]
$\boldsymbol{Q_m}$	Metabolic heat generation	$33800\ W/m^2$	[16]
$\boldsymbol{d_0}$	Displacement amplitude of transducer head	0-182 nm	[6]

IX | Appendix B: Solution Strategy

A. Solver Configurations

Our COMSOL model utilizes three physics modules: the "Helmholtz Equation" module, the "Heat Transfer in Solids" module, and "Domain ODEs and DAEs" module. Configurations for these modules can be found below.

Helmholtz Equation Module

The Helmholtz Equation module was used to solve for the Helmholtz wave equation for the ultrasonic waves in the water and tissue domains. The equation was solved in steady state using pressure as the dependent variable quantity and power flow as the source term quantity. The equation solved using the PARDISO direct solving method.

Heat Transfer in Solids Module

The Heat Transfer in Solids module was used to solve the bioheat transfer equation through the tissue domain based on the various source terms (namely, the ultrasonic source term). This models the Helmholtz equation solution as a dependent variable. The bioheat transfer equation was solved transiently over a period of 10 seconds with 0.1 second time steps. The bioheat transfer equation was solved using the PARDISO direct solving method.

Domain ODEs and DAEs Module

The Domain ODEs and DAEs module was used to implement our thermal dose governing equation. The thermal dose equation was solved transiently over a period of 10 seconds with 0.1 second time steps. The thermal dose equation was implemented as a "Distributed ODE" and was solved using the MUMPS direct solving method. This module was coupled with the heat transfer module in the sense that it utilized the temperature of the tissue domain at every point for each time step. This solver used the same mesh as the mesh used in heat transfer. The thermal dose equation contains a constant that changes based on temperature. To account for this a piecewise function was created that outputs the correct value for the constant depending on the input temperature value.

B. Mesh Design

Two meshes were created in free triangular, one for heat transfer and a second for acoustic pressure. The acoustics mesh can be found in **Figure 6**. The heat transfer mesh can be seen in **Figure 7**. The acoustics mesh must be incredibly fine in order to resolve the different phases of the pressure waves created by the ultrasonic transducer. Thus, for the free triangular region of this mesh, the maximum element size was set to $\frac{c}{6*\omega}$ or one-sixth of the wavelength of the waves [12]. The water and tissue domains are free triangular except for the perfectly matched layer regions, which are mapped distributions. The domain in the perfectly matched layer region needs fewer elements since the waves do not propagate into that region, simulating an open boundary condition emulating tissue. In total, the acoustics mesh has 273,881 total elements. We created a separate, coarser mesh for the heat transfer because it would be computationally unnecessary to have such a fine mesh for the heat transfer domain. Maximum elements size was set to be

0.15 cm in the healthy tissue region and 0.075 cm in the tumor region. The mesh was finer in the tumor region because the tumor region will be the region most subjected to changes in temperature. This mesh has 6,621 total elements.

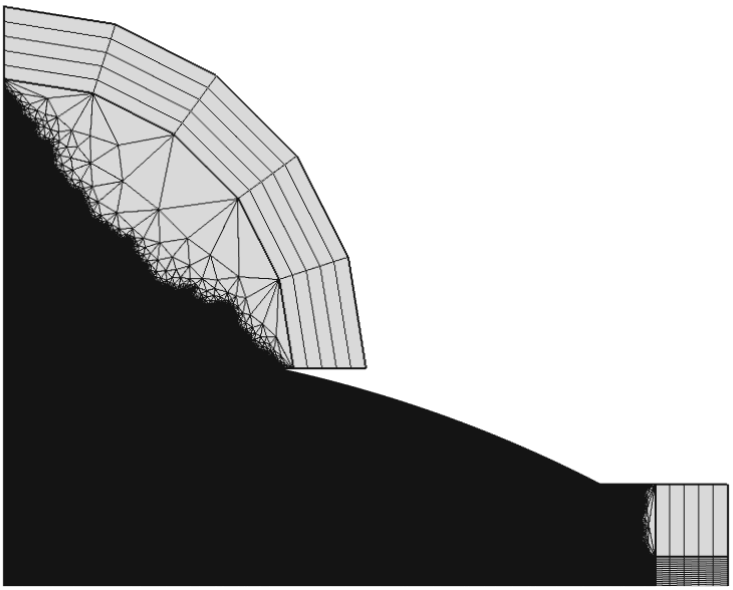

Figure 10. *Close up view of the mesh for our transducer/tissue domain. This mesh is used in conjunction with the Helmholtz module to solve wave propagation through the tissue. Note that the water, tissue and tumor domains are free triangular meshing and the perfectly matched layer region is a distributed mesh. This mesh is made very fine throughout the geometry in order to measure the interaction of pressure waves in the domain, and the steep change in pressure at the transducer site.*

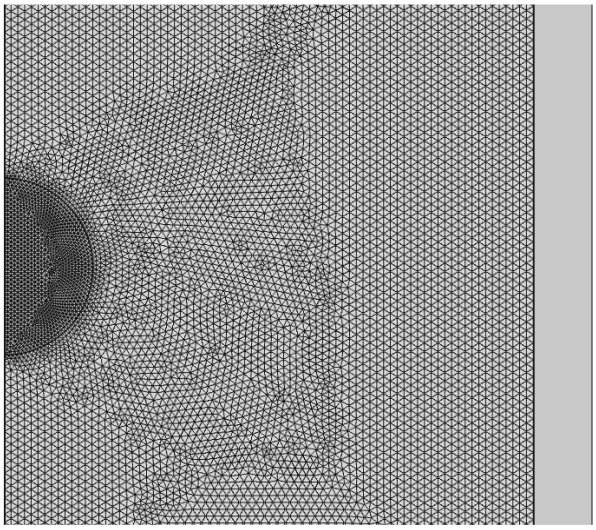

Figure 11. *Close up view of the mesh our tissue and tumor domain. This mesh is used in conjunction with the heat equation to solve heat flow through the tissue and tumor. Free triangular mesh used for heat transfer, maximum element size is 0.150 cm in the healthy tissue and 0.075 cm in the tumor. This mesh maximizes computation at the tumor site where the high heat in tumor ablation can affect healthy tissue, and minimizes computation at distant regions where heat change is less critical*

C. Mesh Convergence Analysis

We performed a mesh convergence analysis on both our acoustics mesh and our heat transfer mesh in order to reduce our discretization error from both sources.

Acoustics Mesh Convergence Analysis

We tracked the average tumor temperature after 4 seconds of sonication while performing a mesh convergence analysis on our acoustics mesh. The temperature of the tumor is relevant to the objective of our study and is also the region most highly subjected to changes in temperature. As such, it is crucial to minimize discretization error in this region. The mesh for our acoustics module needs to be able to fully resolve the ultrasonic waves. This means that the maximum mesh size needs to be a function of wavelength. **Figure 12** shows how average tumor temperature changes as we increase the number of elements in the acoustics domain. The average tumor temperature stabilizes as we reach approximately 273,000 elements. This correlates to a maximum element size of 0.0274 cm which is approximately 1/6th the size of the ultrasonic wavelengths.

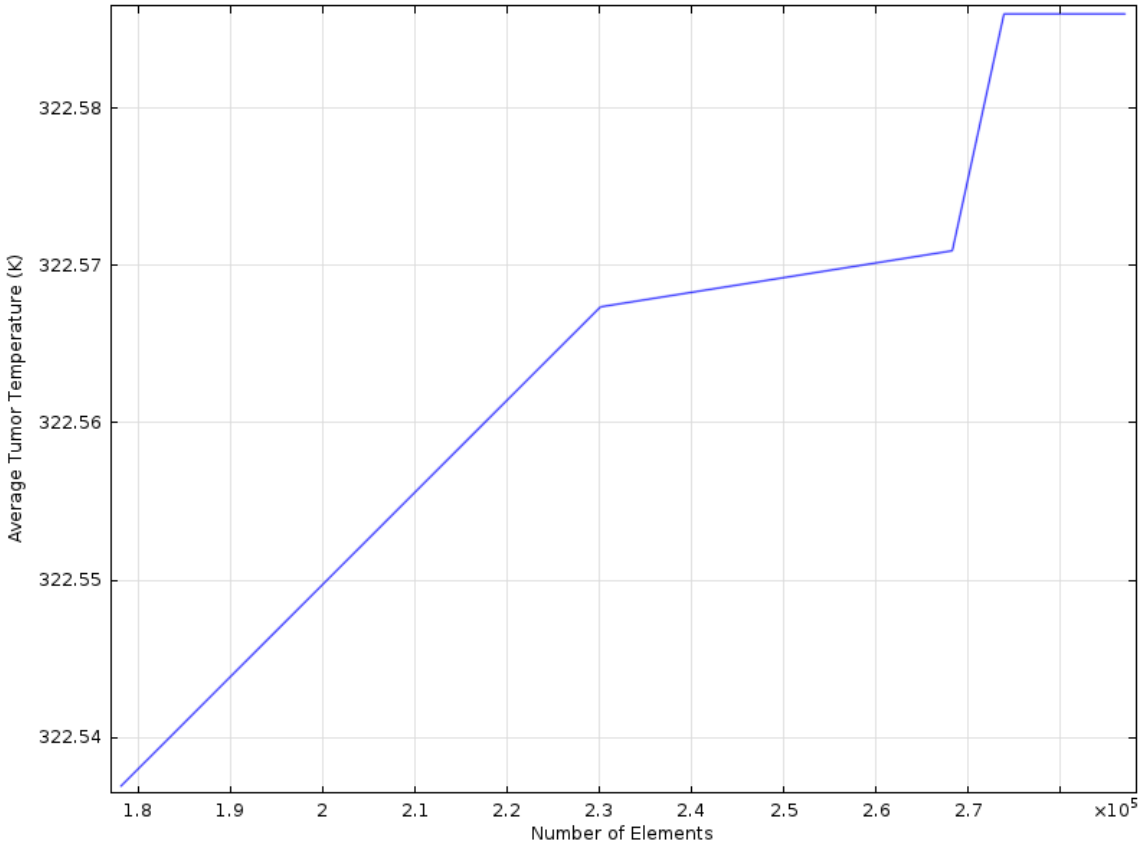

Figure 12. *Average tumor temperature after 4 seconds of heating with varying mesh element sizes. The temperature stabilizes at approximately 273,000 total elements which correlates to a maximum element size of 0.0274 cm. This number of elements is sufficient to reduce discretization error from our acoustics mesh.*

Heat Transfer Mesh Convergence Analysis

We also tracked average temperature of the tumor after 4 seconds of heating while performing a mesh convergence analysis on our heat transfer mesh. **Figure 13** demonstrates the average temperature of the tumor after 4 seconds of heating with varying numbers of mesh elements. It should be noted that we set the mesh in the tumor domain to be twice as fine than the healthy tissue domain. The plot appears to converge once we reach approximately 6600 elements, which corresponds to a maximum mesh element size of 0.15 cm in the healthy tissue and 0.075 cm in the tumor tissue. Using these values for maximum element size will sufficiently reduce discretization error from our heat transfer mesh.

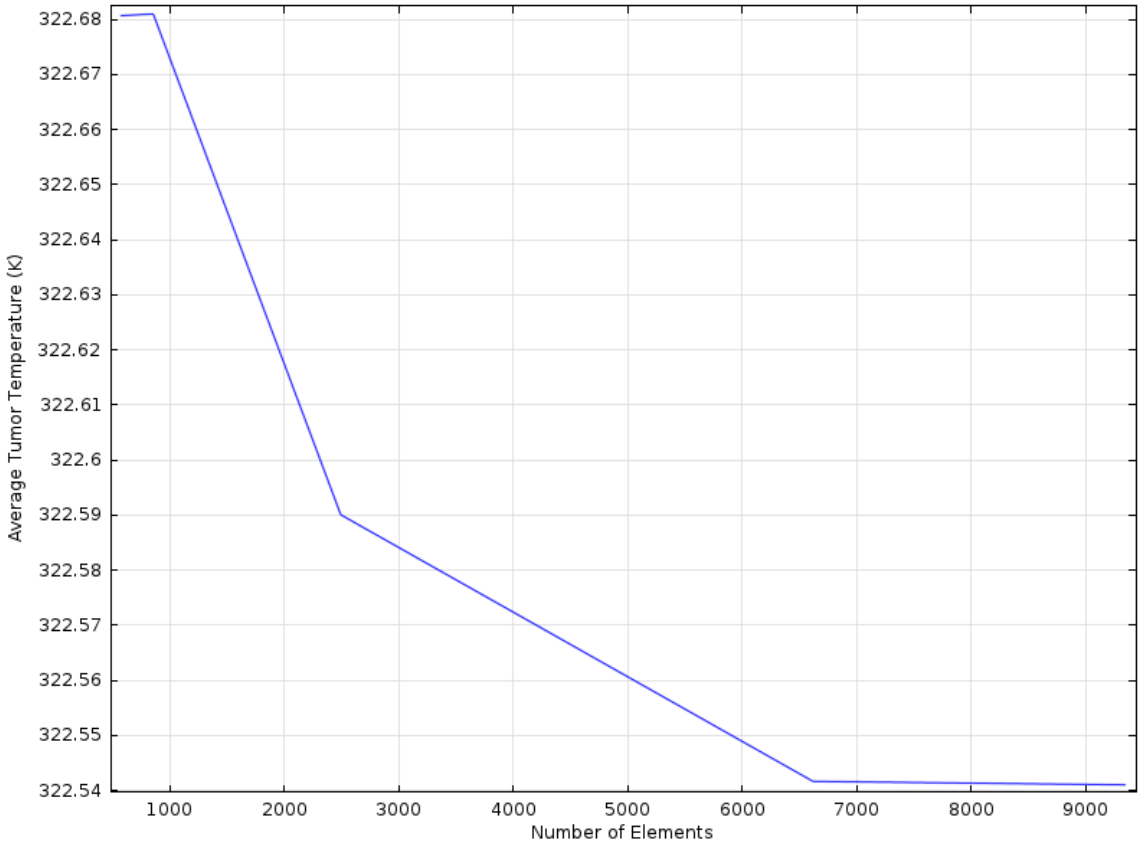

Figure 13. *Average tumor temperature after 4 seconds of heating with varying mesh element sizes. The temperature stabilizes at approximately 6,600 total elements which correlates to a maximum element size of 0.15 cm in the tumor domain and 0.075 cm in the tissue domain. This number of elements is sufficient to reduce discretization error from our acoustics mesh.*

X | Appendix C: References

[1] J.M. Llovet, J. Fuster, J. Bruix. "The Barcelona approach: diagnosis, staging, and treatment of hepatocellular carcinoma." *Liver transplantation*, vol. 10, no. 2, pp. S115-S120. 2004.

[2] R. G. Simonetti, A. Liberati, C. Angiolini, L. Oagliaro. "Treatment of hepatocellular carcinoma: a systematic review of randomized controlled trials." *Annals of Oncology,* vol. 8, no. 2, pp. 117-136. 1997.

[3] "Cirrhosis." Internet: http://digestive.niddk.nih.gov/ddiseases/pubs/cirrhosis/, April 23, 2014 [April 25, 2014].

[4] J.L. Dillenseger, S. Esneault, and C. Garnier. "FFT-based computation of the bioheat transfer equation for the HCC ultrasound surgery therapy modeling." *Engineering in Medicine and Biology Society*. IEEE, 2008.

[5] C.J . Diederich. "Thermal ablation and high-temperature thermal therapy: overview of technology and clinical implementation." *International journal of hyperthermia,* vol. 21, no. 8, pp. 745-753. 2005.

[6] Haifutech Products. *Highfutech* ®. Retrieved 22 February, 2014, from http://www.haifutech.com/index.htm.

[7] "Haifu Model JC Focused Ultrasound Tumor Therapeutic System." *Medical Expo*. Internet: http://news.medicalexpo.com/press/chongqing-haifu-hifu-technology/haifu-model-jc-focused-ultrasound-tumor-therapeutic-system-68035-158334.html, May 16, 2012 [May, 1 2014]. Picture Citation

[8] F. Wu, Z.B. Wang, W.Z. Chen, J.Z. Zou, J. Bai, H. Zhu, K.Q. Li, C.B. Jin, F.L. Xie, H.B. Su. "Advanced hepatocellular carcinoma: Treatment with high-intensity focused ultrasound ablation combined with transcatheter arterial embolization," in *Vascular and Interventional Radiology*. vol. 235, pp. 659-667. May, 2005.

[9] Z.B. Wang, J.Wu, L.Q. Fang, H. Wang, F.Q. Li, Y.B. Tian, X.B. Gong, H. AZhang, L. Zhang and R.Feng. "Preliminary *ex vivo* feasibility study on targeted cell surgery by high intensity focused ultrasound (HIFU)."*Ultrasonics*, vol. 51, pp. 369-375. 2011.

[10] J. C. Bamber and C. R. Hill. "Ultrasonic attenuation and propagation speed in mammalian tissues as a function of temperature." *Ultrasound in medicine & biology* 5.2 (1979): 149-157.

[11] Fujii, Yasutomo, et al. "A new method for attenuation coefficient measurement in the liver Comparison with the spectral shift central frequency method."*Journal of ultrasound in medicine* 21.7 (2002): 783-788.

[12] COMSOL. *Focused Ultrasound Induced Heating in Tissue Phantom*. Retrieved from www.comsol.com.

[13] *Introduction to Acoustics Module.* Internet: http://www.comsol.com/model/download/120903/IntroductionToAcousticsModule.pdf, May 2012, [April 10, 2014].

[14] M.R. Bailey, V.A. Khokhlova, O.A. Sapozhnikov, S.G. Kargi, L.A. Crum. "Physical mechanisms of the therapeutic effect of ultrasound (a review)." *Acoustical Physics,* vol. 49, no. 4, pp. 369-388. 2004.

[15] M.A . Solovchuk, T.W.H. Sheu, M. Thiriet, W.L. Lin, "On a computational study for investigating acoustic streaming and heating during focused ultrasound ablation of liver tumor." *Applied Thermal Engineering,* vol. 56, no. 1 pp. 62-76. 2013.
[16] W. Shen and J. Zhang. “Modeling and Numerical Simulation of Bioheat Transfer and Biomechanics in Soft Tissue.” Mathematical and Computer Modeling, vol. 41, pp. 1251-1265. 2005.